

A Coupling Process of Distillation with Vapor Permeation and Adsorption for Production of Fuel Ethanol: A Comparative Analysis on Energy Consumption

Jiacheng Wang, Jiaqi Zhang, Zhou Hong, Xuechao Gao,* and Xuehong Gu*



Cite This: *Ind. Eng. Chem. Res.* 2022, 61, 1167–1178



Read Online

ACCESS |



Metrics & More

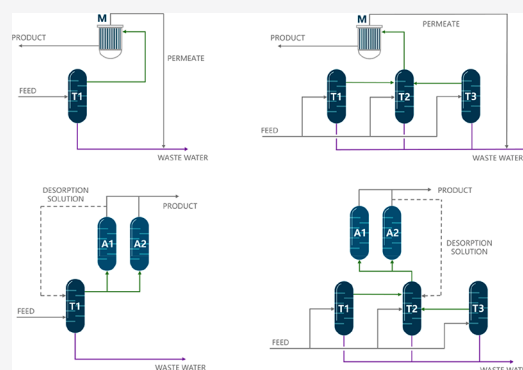


Article Recommendations



Supporting Information

ABSTRACT: To efficiently produce fuel ethanol from fermentation broth, the distillation column was coupled with vapor permeation (VP) of a NaA zeolite membrane instead of using the adsorption technique to remove solvent water. The comparative analysis indicated that the energy efficiency was consistently higher for distillation-VP coupling, using a single-column distillation and three-column distillation, respectively. The best performance was obtained for the VP membrane coupling with a three-column distillation technique, where only 2.7 tons of steam per ton of fuel ethanol were consumed to produce fuel ethanol using a 3.0 wt % ethanol broth. This saved 0.25 tons of steam per ton of fuel ethanol in comparison with the results for the coupling with adsorption technique. The effect of ethanol content in broth on the energy efficiency was also investigated, which indicated that the ethanol content was a decisive factor to determine the energy consumption in the coupling techniques. The operation pressures were crucial to balance the energy consumption between columns coupled with the VP membrane. It was found that the operation pressure of the low-pressure column was the decisive factor to the whole energy efficiency, while the pressure of the high-pressure column was preferably adjusted according to practical production due to fewer disturbances in the system. This work benefits the process design for production of fuel ethanol from fermentation broth.



1. INTRODUCTION

To tackle the environmental issue and energy crisis, fuel ethanol has been widely recognized as a green energy source with significant economic viabilities.^{1–6} In the production of fuel ethanol by biofermentation, plant fiber wastes are the main primary raw material for microorganisms to produce aqueous ethanol solutions.^{7–10} Because of the low presence of ethanol in these aqueous solutions, a large amount of liquid water must be removed to derive a qualified fuel ethanol product. However, the high latent heat of water vaporization in the fermentation broth directly leads to a high production cost of fuel ethanol, so the large-scale production of fuel ethanol remains challenging for industrial manufactures.^{11,12} For instance, when crude oil price reduces, the production of fuel ethanol tends to be inhibited. This is largely caused by the high separation cost of ethanol in the fermentation broth. At present, distillation and pressure swing adsorption (PSA) are combined to achieve this target. However, the high frequency of switching, adsorbent regeneration, and high space volume of equipment reduce the viability of the final product in the market, so it is desirable to find other solutions to further reduce the extraction cost in the production line of fuel ethanol.¹³

Vapor permeation (VP) by membrane is a highly efficient separation methodology, which is particularly suitable for the separation of azeotropic or near-boiling mixtures.^{14–16} Among the membrane candidates, NaA zeolite membranes, with strong hydrophilicities and a well-defined pore framework, exhibited an extremely high separation factor and permeation flux. Since the industrial tubular NaA zeolite membrane plant was first established, significant progress has been made in the field of solvent dehydration.^{17–24} In the past two decades, the VP performance of the NaA zeolite membranes has been significantly optimized in terms of precursor solution, seeding condition, and support microstructure. For instance, to overcome the disadvantage of the moderate permeation flux of the tubular NaA zeolite membrane, a four-channel alumina hollow fiber was developed in our group to replace the tubular support for the growth of the membrane layer. The obtained hollow fiber supported NaA zeolite membrane not only

Received: May 23, 2021

Revised: December 3, 2021

Accepted: December 22, 2021

Published: January 6, 2022



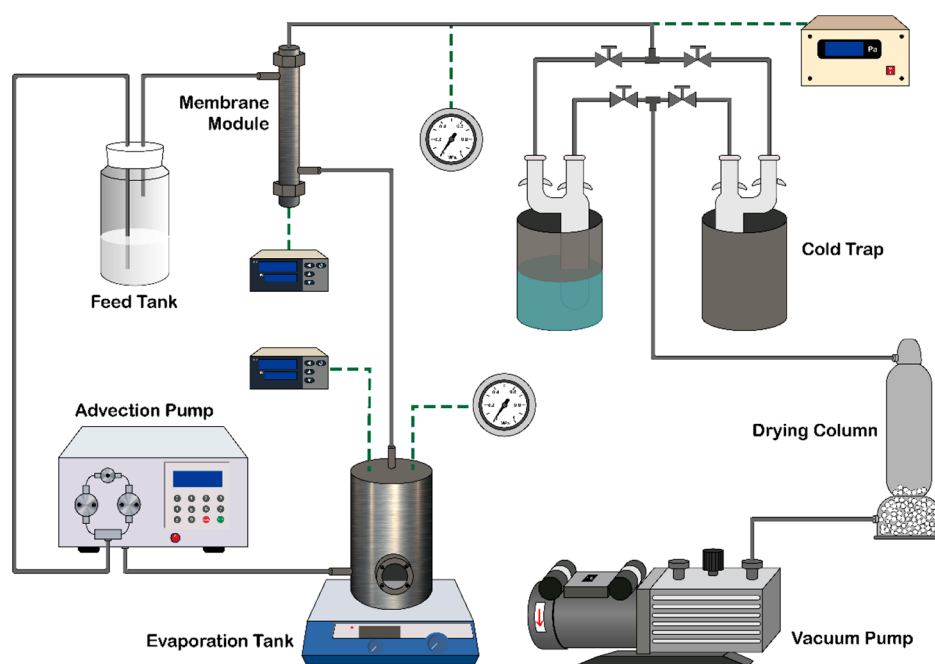


Figure 1. Schematic diagram of the vapor permeation (VP) setup of NaA zeolite membranes for ethanol dehydration.

exhibited ultrahigh permeation fluxes of $12.8 \text{ kg m}^{-2} \text{ h}^{-1}$ and a separation factor of >10000 , but also significantly promoted packing densities by several folds in the membrane module, thereby permitting a much lower facility investment.^{25–27} Apart from the optimization of the membrane performance alone, the dehydration solution could be also explored by combining the membrane process with other separation techniques.^{28,29} This not only avoids membrane contamination but also reduces energy consumption.^{30,31} To produce the anhydrous ethanol, the VP unit could be combined with distillation to accomplish the separation task by balancing the operation parameters between the two units.^{32–34} The industrial combination of the vapor permeation of NaA zeolite membrane and distillation has been successfully achieved.^{35–38} For instance, Harvianto et al.³⁹ proposed the advantages of a cost-effective unit using a coupling distillation-VP unit for isopropyl alcohol (IPA) dehydration, while in our previous work,⁴⁰ it was found that the placement of the NaA membrane unit could enhance the operation flexibility of the column.

Despite the above achievements made by the combination of NaA zeolite membrane with distillation, the coupling process of VP–distillation was still not fully understood for fuel ethanol production. For instance, most of the work in the literature was largely about the feasibility validation for a simple process, for which a single column was coupled with a membrane unit alone, so the specific comparison of energy consumption and operation conditions between different coupling techniques was missing. In addition, the ethanol concentration in the feeding to the distillation column was fixed to be above 20 wt %, so the derived analysis could not be directly used to produce fuel ethanol from the fermentation broth, where a low concentration of ethanol is involved. This inconvenience was caused by the unattended relationship between operation parameters and separation efficiency. To address the above issues, this work examined different coupling processes of distillation with the adsorption or VP to produce a standard fuel ethanol product from fermentation broths with low ethanol contents based on a gas fermentation technique

using CO and N₂. On the basis of a single and multieffect distillation and a practical membrane block in Aspen plus, the relationship between the energy efficiencies and internal operation conditions (feed concentration, split ratio, and operation pressure) were extensively estimated and compared between the two techniques. To our best knowledge, this is the first systematic study on the distillation-VP coupling process, considering multieffect distillation, operating parameters with feed concentration, split ratio, and operation pressure. The membrane model was validated against VP data from Jiangsu Nine Heaven High-Tech Co., Ltd. by characterizing a tubular zeolite membrane used in its own membrane equipment, applying a 3 wt % ethanol feed broth for a production capacity of 20 000 tons per year.

2. MEMBRANE PERFORMANCE CHARACTERIZATION

Before the coupling process, the membrane performance was characterized. Figure 1 depicted the VP setup of the NaA zeolite membrane for ethanol dehydration.⁴¹ The tubular NaA zeolite membrane was applied in this study, which was produced with a length of 80 cm, an external diameter of 12.5 mm, and an internal diameter of 8 mm. The effective area of the tubular membrane used for the experiments was 0.03 m^2 . The permeation flux was $1.8 \text{ kg m}^{-2} \text{ h}^{-1}$ under the operation pressure of 0.1 MPa with a feed concentration of 90 wt % ethanol at 100 °C, and the separation factor was 400. As suggested, the evaporated feeding flow was directed into a NaA membrane module, where the feed pressure could be adjusted between 1 and 4 barg, the corresponding temperature ranged from 103 to 137 °C, and the feed flow rate was set to be 100 mL/min. The permeate was extracted by a vacuum pump and collected by cold traps (liquid nitrogen) to maintain a low-pressure of 1000 Pa. The purities of the feed and permeate were analyzed by a Karl Fischer moisture meter (Mettler Toledo DL-31) and a gas chromatography (GC-2014, Shimadzu) equipped with a packed column of Parapak-Q. The membrane performances were evaluated by flux (J_i) and separation factor (α), respectively:

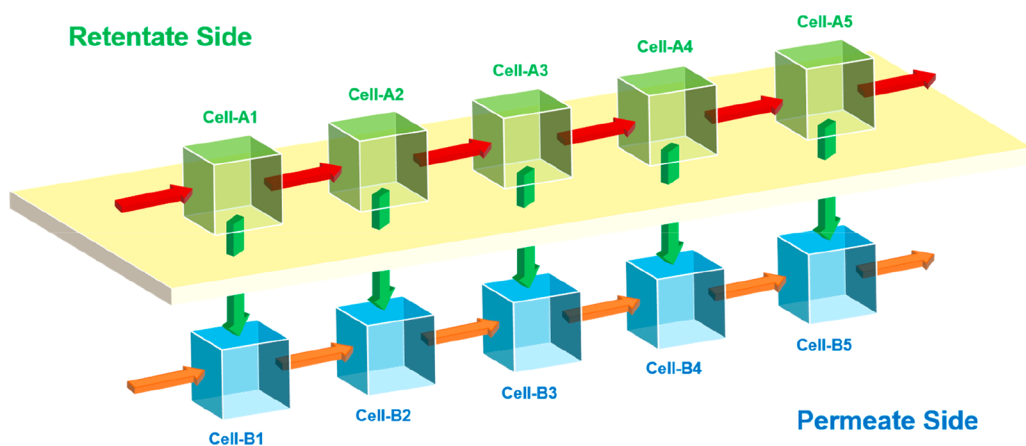


Figure 2. Schematic diagram of VP membrane blocks in ACM.

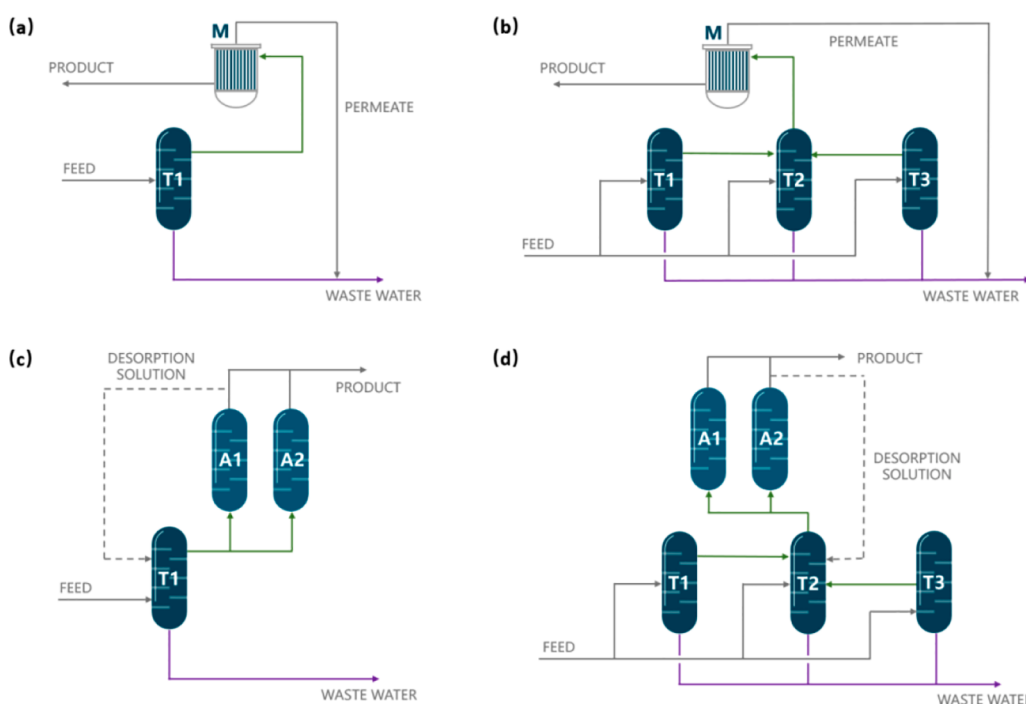


Figure 3. Schematic drawings of four different couplings to produce fuel ethanol, (a) single-column distillation with membrane process (1-DISTL VP), (b) three-column distillation with membrane process (3-DISTL VP), (c) single-column distillation with pressure swing adsorption (PSA) process (1-DISTL AD), (d) three-column distillation with PSA process (3-DISTL AD)

$$J_i = \frac{m_i}{At} \quad (1)$$

$$\alpha = \frac{Y_W/X_W}{Y_E/X_E} \quad (2)$$

where m_i is the collected mass of the permeate i , kg, under an operating time interval of t , h; A corresponds to the effective membrane area, m^2 ; X_W/Y_W and X_E/Y_E are the mass fractions of water and ethanol in the feed/permeate, respectively.

3. MODELING AND SIMULATION

3.1. Modeling of the Membrane Performance. The Aspen custom modeler (ACM) provides an efficient method for chemical process design to create a customized block by defining governing equations.^{42–45} In this work, a plug flow was used for the VP membrane block. To combine the ACM

equation with the VP membrane performance,^{46–49} a semi-empirical expression with two parameters was proposed:

$$J_i = k_i \exp\left(\frac{-E_i}{RT}\right)(x_F p_F - y_P p_P) \quad (3)$$

where E_i and k_i represent the thermal parameter in Arrhenius form and pre-exponential factor of each component, respectively, which could be estimated based on the fitting of experimental data. Figure 2 depicted the schematic diagram for the NaA zeolite membrane equipment in the ACM, where the membrane block was divided into 10 pairs of discrete cells, with the mass transfer equation in each cell described as

$$F_{RI}Z_{RI,i} = F_{RO}Z_{RO,i} + F_M Z_{M,i} \quad (4)$$

$$F_{PO}Z_{PO,i} = F_{PI}Z_{PI,i} + F_M Z_{M,i} \quad (5)$$

Table 1. Operational Parameters of Distillation Columns in Different Coupling Processes

parameters	1-DISTL VP		3-DISTL VP		1-DISTL AD		3-DISTL AD	
	T1	T1 (LP)	T2 (MP)	T3 (HP)	T1	T1 (LP)	T2 (MP)	T3 (HP)
no. of theoretical stages	40	28	28	40	40	28	28	40
feed stage	30	1	1	20/30	15/30	1	1	15/25/30
operation pressure (barg)	4	-0.6	0	4	3	-0.6	0	3
feed concentration (wt %)	3	3	3	26/3	70/3	3	3	70/26/3
top concentration (wt %)	85.5	26	26	85.5	92	26	26	92

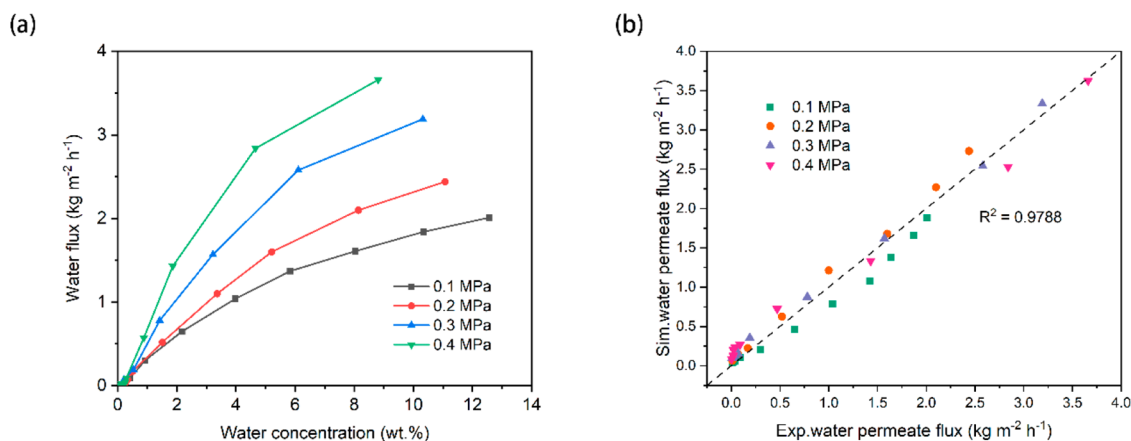


Figure 4. (a) Variation of permeation flux with water concentration in the feed; (b) comparison of water flux between the experimental measurements and simulated results in ACM.

where F and Z_i represent the flow rate and the composition of component i of the flow. The subscripts RI, PI, RO, and PO represent the input and output flow of the retentate and permeate side, respectively. The total membrane area was determined by the number of cells, while the total flux for the VP block was calculated by

$$F_M Z_{M,i} = N \Delta A \cdot J_i \quad (6)$$

After compiling, the VP membrane block could be embedded in Aspen Plus, and the separation capacities could be adjusted by changing the cell number in the user interface.

3.2. Process Simulation. Figure 3 provides four different couplings for production of fuel ethanol from fermentation broth (3.0 wt % ethanol), where the VP membrane or adsorption block coupled with the distillation column to yield the final product flow (99.5 wt % ethanol), which is a typical concentration for fuel ethanol. In the process simulation, the influences of multieffect distillation, operating parameters, feed concentration, split ratio, and operation pressure on the energy consumption were systematically examined. The production capacity was maintained at 20 000 tons per year in all cases according to the plan for ethanol plants with gas fermentation technology, where the feed gas was CO and H₂ provided by Jiangsu Nine Heaven High-Tech Co., Ltd. Compared with the classic fermentation process based on starch to produce bioethanol, the significant advantage of the gas fermentation process is food saving.^{50,51} On the other hand, the gas fermentation process yields a much lower ethanol concentration in broth as compared to the conventional starch fermentation process, which could yield a high concentration of 15 wt %.^{52,53} Since the feed gas was CO and H₂ in the gas fermentation process, the dissolved CO₂ is very limited, which was neglected in the system due to its negligible influence on energy consumption, as shown in the Supporting Information.

However, the dissolved CO₂ in the feed should be included for realistic and practical studies. In Figure 3a, the feed was directly flowed into a single column to derive a distill of 85.5 wt % ethanol before entering the VP membrane block (1-DISTL VP) based on the general concentration requirement for feed in the specific VP process. A three-column distillation technique has been developed for the recovery of ethanol, and significant promotion has been achieved for the product quality and energy efficiency.^{54,55} Compared with a single column distillation, it is known that both the operation difficulty and facility investment for a multieffect distillation are higher, so we also examined 1-DISTL VP and 1-DISTL AD in the process comparison, where the compromise of the different processes can be further studied especially from the perspective of energy cost. As given in Figure 3b, the broth feed was divided into three substreams before entering the columns operated at low-pressure (LP), medium-pressure (MP), and high-pressure (HP), respectively. Meanwhile, the two distills (26 wt % ethanol) from LP and MP columns were then combined to enter the HP column, in which the vaporous flow with a purity of 85.5 wt % ethanol from the HP column provided the feed for the VP membrane block (3-DISTL VP). For the three columns, the multieffect distillation was also applied to reduce the energy consumption, where the condenser operating at lower pressure was thermally balanced with the reboiler operating at higher pressure. By setting the required design specifications, the energy matching can be achieved by iterations of the two split ratios for the feed flow in the process, so only the HP column consumed energies. The same procedures were also applied for the adsorption technique. As depicted in Figure 3c, a single column and a closed-cycle batch PSA system were combined to produce fuel ethanol (1-DISTL AD), where the desorption flow was used for the regeneration of the adsorbent. According to the

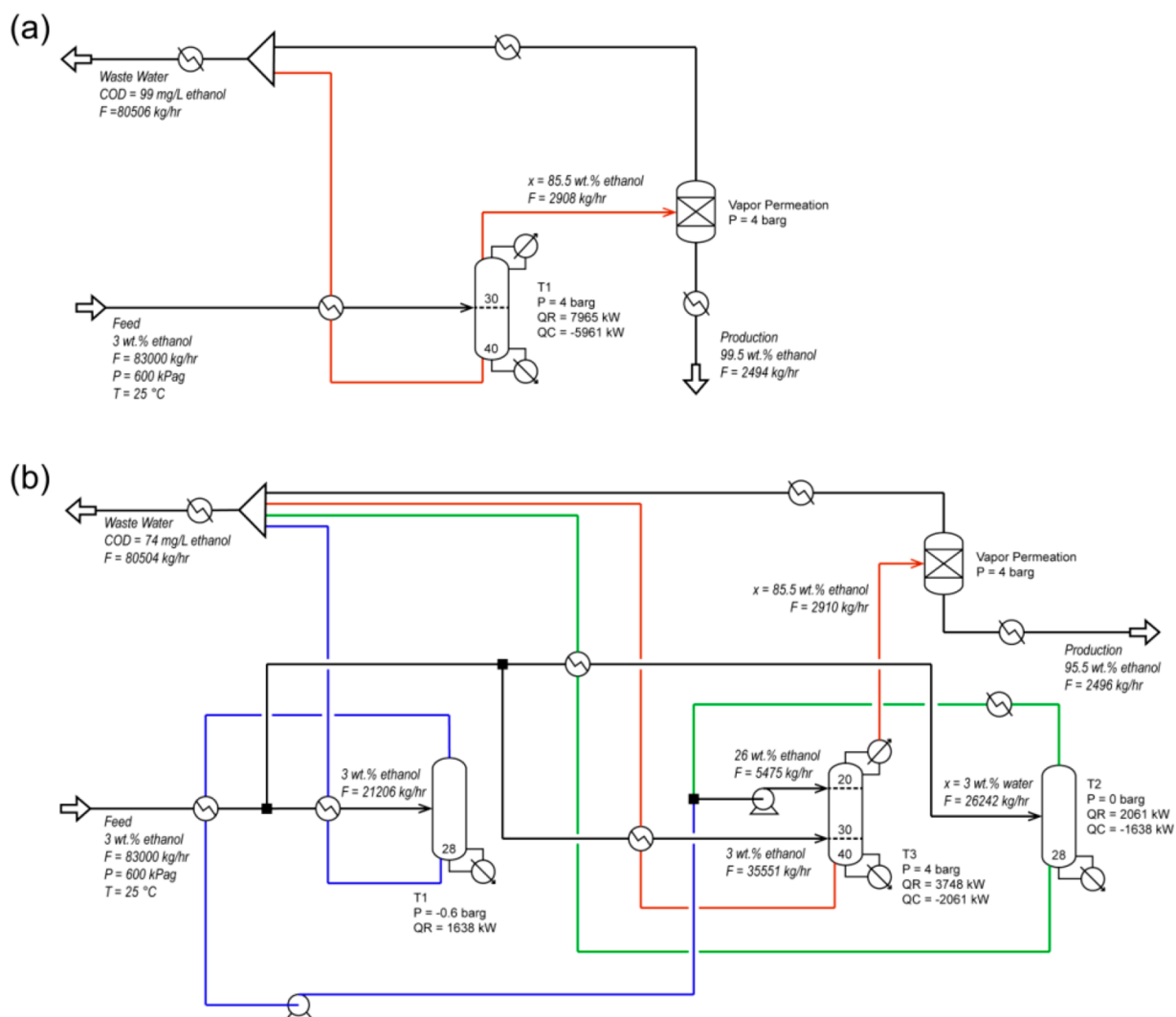


Figure 5. Production flowsheets of fuel ethanol based on the coupling of the VP membrane with (a) single-column distillation technique and (b) multieffect distillation technique, respectively, in which the ethanol content in the wastewater was below 0.01 wt %.

experimental data,⁵⁶ a 92 wt % ethanol vaporous distill from the column was directed into the PSA process. For the multieffect distillation in Figure 3d, the procedure was similar (3-DISTL VP), where the broth feed was partitioned into three substreams among columns with different pressures to balance the energy consumptions. A 92 wt % ethanol distill from the HP column was obtained to feed the PSA block, and a sweep flow with 70 wt % ethanol was extracted and then redirected into the HP column in the desorption section. The permeating and bottom streams in all the couplings were treated as wastewater with ethanol content below 0.01 wt %. In addition, the applied VP membrane was a tubular NaA zeolite membrane. Compared with the newly developed hollow fiber zeolite membrane, a tubular NaA zeolite membrane has a lower permeation flux, so a high membrane area is used, whereas the energy duty remains the same. The main operation parameters for each column in different couplings were summarized in Table 1. The NRTL-RK equation of state with Henry's law was applied in the simulation.

4. RESULTS AND DISCUSSIONS

4.1. Validation of Transport Model in ACM. To validate the accuracy of mass transfer equation given in eq 3, the NaA

zeolite membrane was characterized by dehydrating an ethanol/water mixture using vapor permeation, for which the operation pressure was adjusted between 0.1 and 0.4 MPa. The relationship between flux and water concentration was plotted in Figure 4a, where the dependence of flux on water content could be explained by the adsorption behavior of water in NaA zeolite.^{24,57} Because the dehydration experiments were conducted in a cycling dehydration process, the separation factor is exclusively determined by the water purity in the permeate. To dehydrate a 15 wt % water/ethanol mixture, the obtained water purity in the permeate was about 99.97 wt %, so the separation factor was about 588. The permeation data were correlated according to the transport equation of eq 3, where the simulated values of k and E were $0.679 \text{ kg}\cdot\text{m}^{-2}\cdot\text{h}^{-1}$ and $616.624 \text{ J}\cdot\text{mol}^{-1}$, respectively. The comparison of water flux between the experimental measurement and model prediction in ACM was depicted in Figure 4b. It was seen that the average R^2 value reached up to 0.98, indicating good agreement between the two results.

4.2. Flowsheet Optimization of the Four Couplings.

In the process simulation by Aspen Plus, all the operation parameters were defined and optimized to minimize the energy cost. The flowsheets of the VP membrane block coupled with

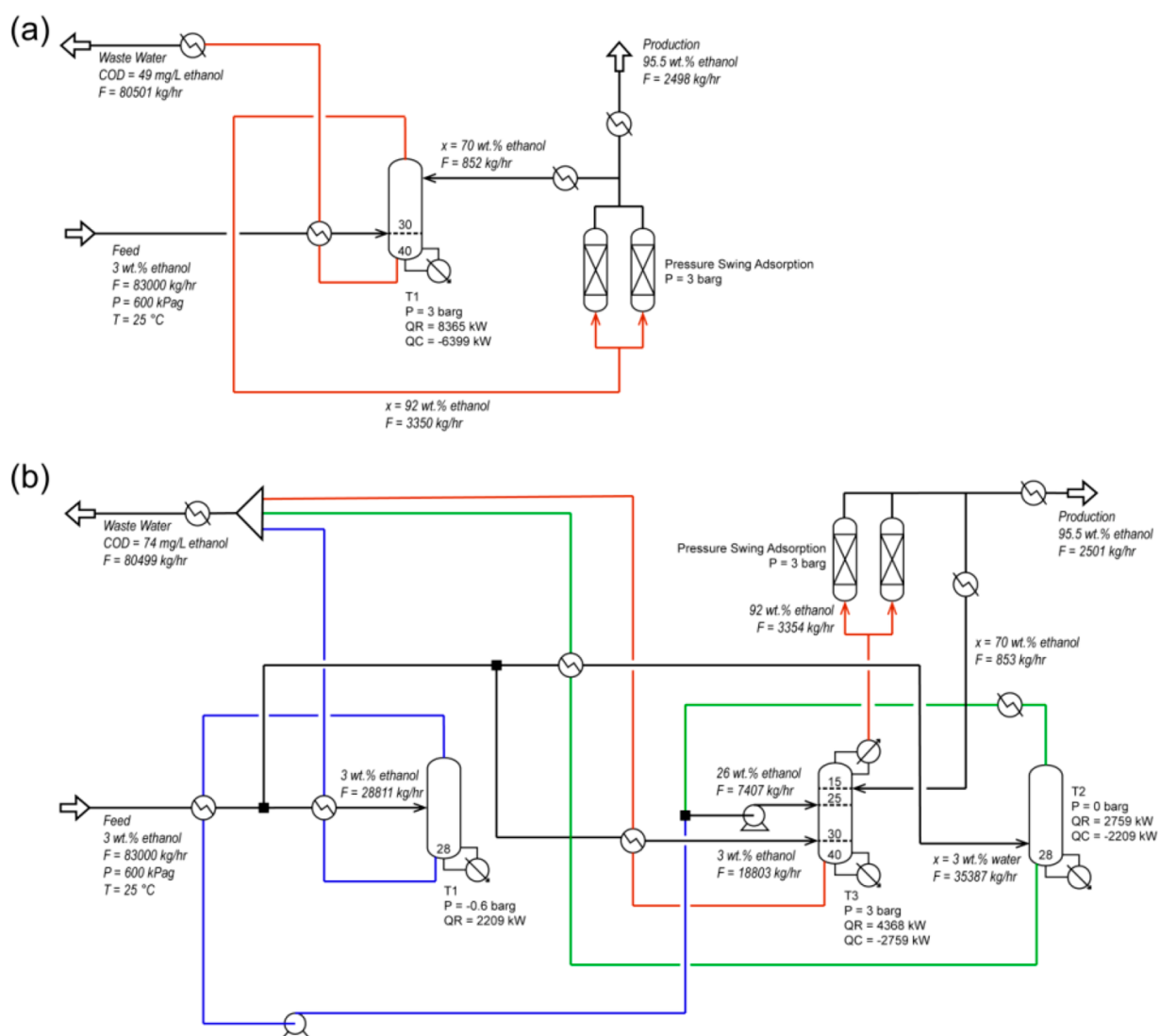


Figure 6. Production flowsheets of fuel ethanol based on the coupling of the PSA section with (a) single-column distillation technique and (b) multieffect distillation technique, respectively, in which the ethanol content in the wastewater was below 0.01 wt %.

the single-column distillation or three-column distillation were shown in Figure 5. As suggested in Figure 5a, the heat duty for the single-column distillation coupling was high, up to 7965 kW. By comparing with the results for the alternative based on three-column distillation in Figure 5b, the heat consumptions of the LP, MP, and HP columns corresponded to 1638 kW, 2061 kW, and 3748 kW, respectively. Since the multieffect distillation technique was applied, the total heat consumption in the three-column distillation was only 3748 kW, so there was a 52.9% heat saving. Compared with an energy consumption of 4908 kW in the conventional three-column configuration of extractive distillation without any heat integration process,^{33,58} energy consumption could be saved by 18.7% under the same feed characterization, a feed flow of 1694.24 kmol h⁻¹ with ethanol mole fraction of 5%. Similarly, the energy efficiency could be also promoted by process intensification with heat integration, where at least 20% of energy consumption could be saved. Figure 6 depicted the flowsheets of the adsorption block coupled with a single-column distillation or three-column distillation. For the single-column distillation coupling with PSA block a in Figure 6a, the heat duty was slightly higher in comparison with the result for

the single-column coupling with the VP membrane in Figure 5a (8365 kW versus 7965 kW), which led to a saving percentage of 4.8% for the membrane coupling. The small difference suggested that the advantage of the VP membrane was insignificant for single-column distillation couplings. On the contrary, if multieffect distillation was used with PSA block in Figure 6b, the heat consumptions corresponded to 2209 kW, 2759 kW, and 4368 kW for the columns operated under LP, MP, and HP conditions, respectively. By canceling out the heat consumptions of the LP and MP columns, the saving percentage of heat in the multieffect distillation was about 47.8%, compared with the result based on a single column technique in Figure 6a. The ethanol losses of each process are 4.03 kg/h (0.16%) for the 1-DISTL AD process, 8.14 kg/h (0.33%) for the 1-DISTL VP process, 2.09 kg/h (0.8%) for the 3-DISTL AD process, and 2.21 kg/h (0.9%) for the 3-DISTL VP process, respectively. Further, by comparing with the multieffect distillation results between VP membrane and PSA couplings, the advantage of the VP membrane became more significant: the percentage drop of heat consumption was increased up to 14.2%, being much higher than the value of 4.8% derived for the comparison between single column

Table 2. Detailed Comparison of Energy Consumption in the Coupling Process with VP Membrane and Adsorption Techniques

parameters	1-DISTL VP	3-DISTL VP	1-DISTL AD	3-DISTL AD
heating duty for membrane/adsorption, kW	23	23	26	26
cooling duty for permeate/desorption, kW	−264	−264	−320	−318
total cooling duty, kW	−6391	−2539	−6659	−2888
total heating duty, kW	7988	3771	8391	4394
steam consumption, t/t	5.42	2.73	5.68	2.98
recycle water consumption, m ³ /t	230	84	240	128
cooling water consumption, m ³ /t	10	10	11	11
electricity consumption for pumps and vacuum, kW	25	30	20	25

distillation couplings. It is noted that there is a minor feeding pressure difference between the PSA and VP membrane unit in the process simulation, and this was due to the different setting requirements in the practice operation, in which a higher feeding pressure for the VP membrane unit could reduce the required membrane area.

The above comparisons were discussed above the heat energies of the columns among different couplings alone, which should be further compared with the energy consumptions in other units and parts of the flowsheet (see the [Supporting Information](#) for the detailed information of all the streams in the four couplings). The detailed energy cost correlated with the utilities of steam, water usage, and electric cost for different sections in the coupling processes were summarized [Table 2](#). It is noted that the ethylene glycol or saline cooling water was used to condense the permeate vapor in the VP process operated at 2000 Pa, which was a typical setting in an industrial application. In the condenser for the permeate, the temperature at the inlet of cooling water is −5 °C, and the temperature at the outlet of cooling water is about 0 °C. For the hot side, the inlet of water/ethanol vapor (hot side) is about 30–40 °C, while the outlet of water/ethanol liquid (hot side) is about 5 °C. The energy cost for reboilers and condensers were generated by Aspen Plus, and the electricity costs for pumps and vacuum were provided from the product supplier according to the required flow capacity and vacuum degree. As shown, comparing with water usage and electric cost, most of the total energy cost in the entire coupling process was contributed by steam consumption, so this parameter could be used to represent the production efficiency in different couplings. For a single-column distillation coupling with VP membranes, the steam consumption was 5.42 tons per ton of product, which was reduced to 2.73 tons per ton of product in the multieffect distillation coupling with VP membranes. By comparison, the steam consumptions for the PSA coupling with single-column distillation and multieffect distillation corresponded to 5.68 and 2.98 tons per ton of product, respectively, so 0.25 tons of steam could be saved if the PSA technique was used instead of the VP membrane technique. The higher energy efficiency of the VP membrane coupling was attributed to two main advantages in the VP membrane-based process; that is, (i) the separation ability of the VP membrane is very high, so the water content in the feed flow (85.5 wt %) from the HP column could be much higher than that for the HP column in the PSA coupling (92 wt %); (ii) no sweeping steam was involved in the VP coupling, so a lower reflux ratio was used in the column.

4.3. Effect of Ethanol Content in Broth on the Steam Consumption. Since the ethanol content in broth was

affected by the fermentation techniques, so the influence of ethanol content in broth on the steam consumption should be also explored to facilitate the application of the separation coupling. Such a plot was provided in [Figure 7](#). As expected,

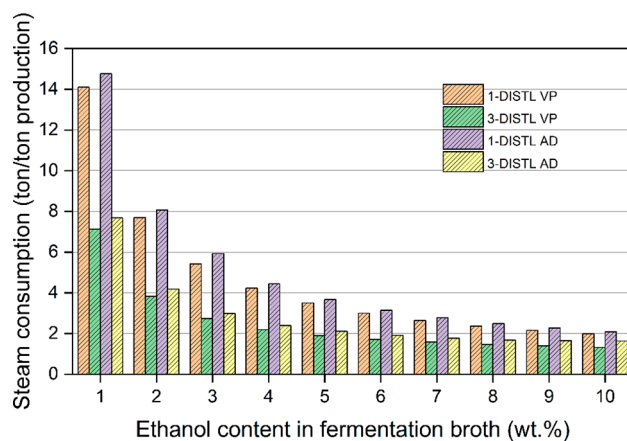


Figure 7. Comparison of the steam consumption with different ethanol contents in fermentation broth for VP and AD coupling with single and multieffect distillations.

higher steam consumption occurred to lower ethanol content values, where more water liquid should be evaporated in the distillation. For the single-column and multieffect column distillation coupled with VP membranes, the steam consumption could be as high as up to 14.1 and 7.12 tons per ton of product, respectively, when the ethanol content in the broth was low, up to 1.0 wt %. Meanwhile, the steam consumption only marginally decreased when the ethanol content reached a threshold (5.0 wt %), suggesting no significant promotion effect after this boundary. For the coupling processes with PSA in [Figure 7](#), the variation of steam consumption was also similar, except there is a consistently higher value in comparison with the result for the VP membrane. Depending on the ethanol content, the steam consumption varied from 14.76 and 7.68 to 2.9 and 1.63 tons per ton of product for the single column coupling and multieffect column coupling, respectively. The above results indicated that the ethanol content in broth was a decisive factor to determine steam consumption in the coupling process.

To understand the influence of the ethanol content on energy consumptions in the multieffect column distillation, the split ratios of FS1 and FS2 were extracted to provide the feeding flow for LP and MP columns, in which the value of FS2 represented the partition of the feed from the FS1 splitter. The values of the two split ratios are the variables for achieving the design specifications of the target concentration for the top

and bottom output of the HP column. Both ratios have been optimized in such regulations. Such a plot was provided in Figure 8. As the figure suggests, both the split ratios of FS1 and

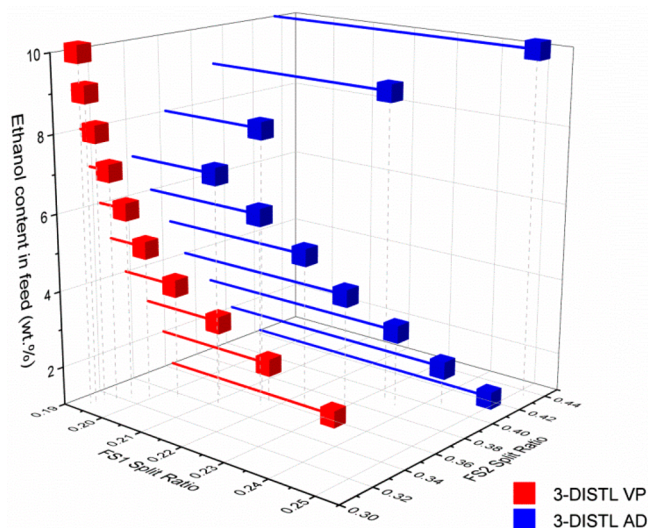


Figure 8. Dependence of split ratios for FS1 and FS2 on ethanol content in fermentation broth for VP or AD coupling with multieffect distillation.

FS2 consistently decreased with the increment of ethanol content for the whole VP coupling range. This indicated that the LP and MP columns are mainly used for the initial enrichment of ethanol from the crude fermentation broth, while the HP column acted as the refinery to provide feed for the VP unit. By comparison, the split ratios of FS1 and FS2 in the PSA coupling process decreased with the increment of ethanol content until 7 wt %, suggesting the load for the HP column became higher. However, to further increase the ethanol content, a turning point occurred, in which the FS1 split ratio in the PSA coupling started to increase, suggesting the load for the LP column became higher. The enhanced load for the HP column could be attributed to the increase in the sweep flow, which was used for the regeneration of the adsorbate in the PSA technique.

4.4. Effect of Operation Pressures in LP and HP Columns. Figure 9 analyzed the effect of the operation pressure of LP and HP columns on total heating duty. As suggested, if the operation pressure of the LP column was fixed at -60 kPag, the total duty only increased slightly from 2.72 to 2.74 tons of steam per ton of production, along the increases in the operation pressure of the HP column from 300 to 550 kPag. Alternatively, if the HP column was fixed at 400 kPag, a much stronger increment (nearly 0.2 tons of steam) occurred, when the operation pressure of the LP column was adjusted from -60 kPag to -10 kPag, suggesting the operation pressure in the LP column was the decisive factor to determine the total energy consumption. In practice, the operation pressure of the HP column should be determined in advance to fulfill the requirement for the VP membrane, where the feeding pressure should be sufficiently high to provide a high yield rate of the water in the permeate side. Since the energy-saving in multieffect distillation is about the heat balancing among columns under different pressures, the key measure to reduce the total energy consumption was to set the operation pressure of the MP column as small as possible. Such a setting could

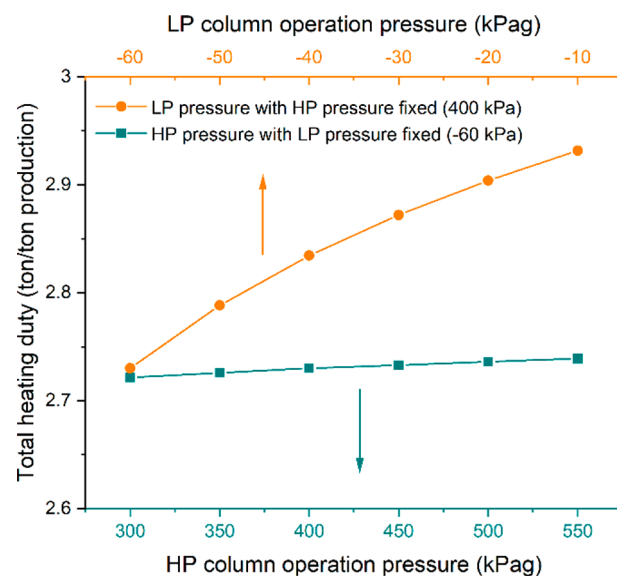


Figure 9. Total heating duty dependence on column pressure, where the yellow line represents the variation of total heat duty with an operation pressure of the LP column under a fixed pressure in the HP column (400 kPag), while the green line represents the variation of total heating duty with the operation pressure of the HP column under a fixed pressure in the LP column (-60 kPag).

eventually lead to the operation pressure for the LP column as low as possible to balance the heat exchange with the MP column, thereby reducing the total energy cost as much as possible. In addition, to reduce the facility investment for VP membrane, the driving force across the membrane should be sufficiently high, so a value of 4 barg was recommended for the operation pressure in the HP column.

To explore the relationship between the energy consumption and operation condition of the columns, both the split ratios of FS1 and FS2 under different operation pressures were extracted. Such a plot was provided in Figure 10a,b, using a fixed pressure in the HP column and LP column, respectively. As suggested, with the decrease in the pressure of an LP column, a systematic decreasing pattern occurred to both split ratios. By comparison, the decrease in the split ratio of FS1 was much more significant, while the split ratio of FS2 only decreased marginally in both cases. This suggests that it is preferable to adjust the HP column pressure in practical production, as the changes in splitting valves (FS1 and FS2) are minor, leading to less flow disturbance for the full process.

The above conclusion could be further supported by the mass flow details inside the columns, as provided in Figures 11 and 12, in which mass flow rates at the tops and bottoms for all the columns are illustrated to find the key factor affecting the separation process, which is related to the energy consumption. As shown in Figure 11a, with the increase in LP column pressure from -60 kPag to -10 kPag, under a fixed pressure in the HP column, the mass flow rates from the top of the HP column were maintained at 2910 kg h^{-1} . This is due to the rigid requirement for VP membranes, for which the feeding concentration of ethanol from the distill was fixed at 85.5 wt %. In addition, the flow rate at the MP column top sustained a slight increase; but the results at the LP column top were significantly decreased from 2074 kg h^{-1} to 1660 kg h^{-1} , suggesting that more flow disturbances in the LP column were expected in the system during the adjustment. For the mass

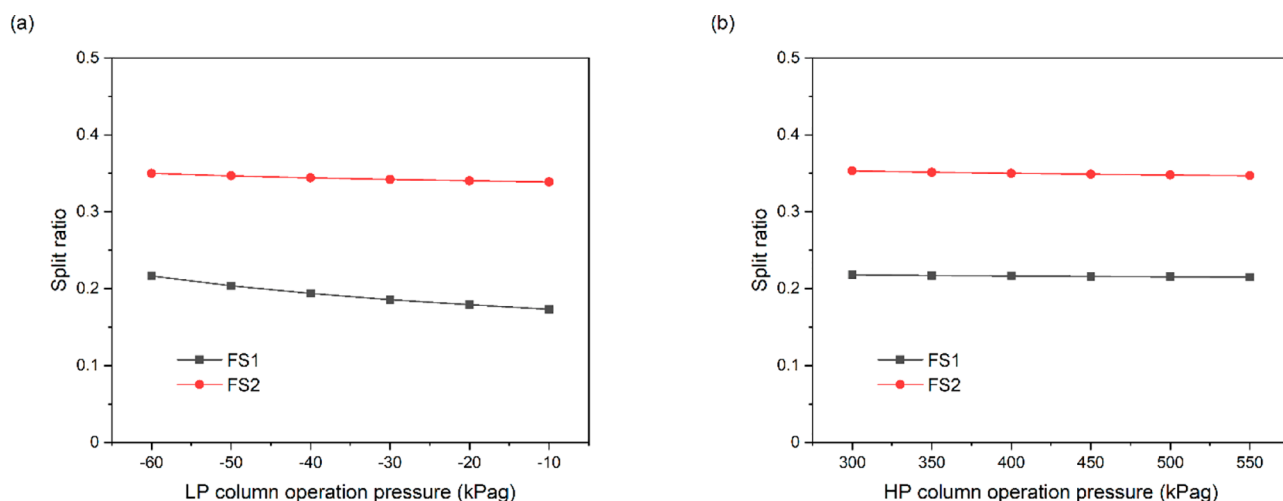


Figure 10. Split ratio dependence on column pressure: (a) split ratio versus operation pressure of LP column under a fixed pressure of HP column (400 kPag), (b) split ratio versus operation pressure of HP column under a fixed pressure in LP column (−60 kPag).

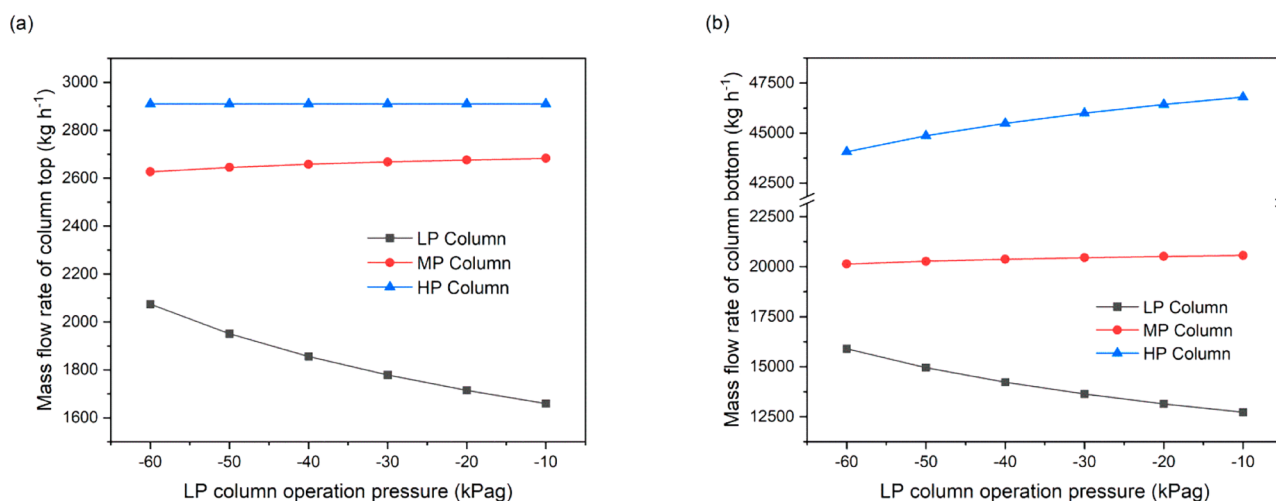


Figure 11. Variation of mass flow rate in the columns with pressure settings in the LP column, under a fixed operation pressure setting in the HP column (400 kPag): (a) top and (b) bottom.

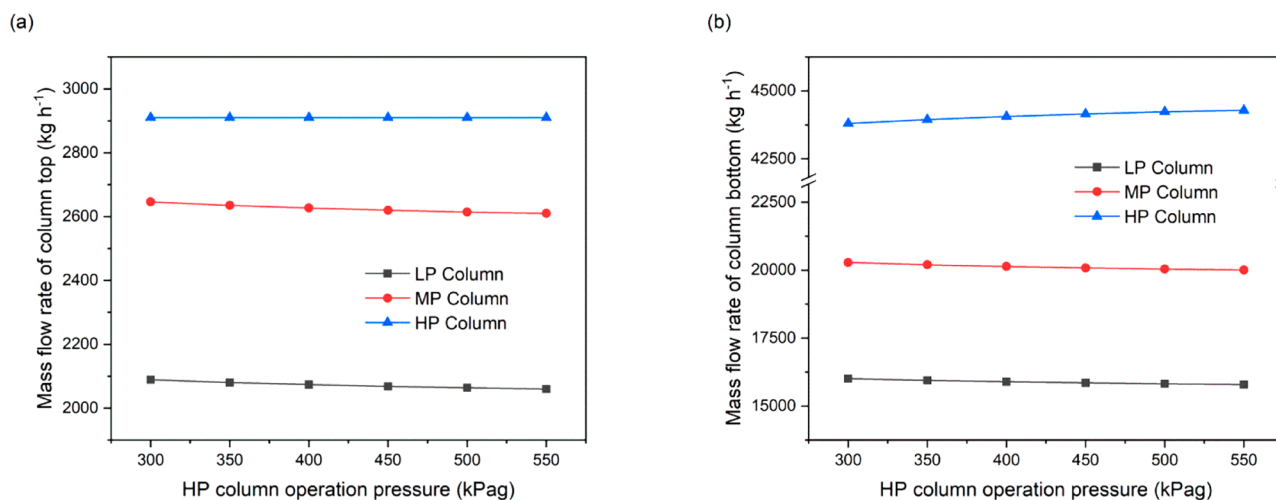


Figure 12. Variation of mass flow rate in the columns with pressure settings in HP column, under a fixed operation pressure setting in LP column (−60 kPag): (a) top and (b) bottom.

flow rates at the column bottoms in Figure 11b, the dependences were similar for MP and LP columns, where an

almost constant tendency and a decreasing tendency were seen, respectively. On the contrary, the mass flow rate at the

HP column rose sharply from 44059 kg h⁻¹ to 46796 kg h⁻¹, so more flow disturbance also occurred in the HP column. These results indicated that the flow conditions in both the LP and HP columns were significantly affected by the operation pressures between columns, so the full process should take more time to stabilize under a new pressure setting. By comparison, Figure 12 depicted the variation of mass flow rates at the tops and bottoms for all the columns versus operation pressures in the HP column, when the operation pressure of the LP column was fixed. As suggested, the overall variation was insignificant for all the conditions, so the influences of operation pressure of the HP column on the flow condition in all the columns were negligible, indicating the full process should take less time to become steady under a new operation pressure setting.

On the basis of the comparison between Figures 11 and 12, it is readily concluded that the adjustment of the HP column is preferred according to practical production, when it is necessary.

5. SUMMARY AND CONCLUSION

The coupling of distillation and the VP membrane could yield significant advantages in alcoholic dehydration. However, this effect was still not fully understood as most of the work was focused on a feasibility test and validation of the coupling, and only a simple parameter was monitored. This is largely caused by the inconveniences that occur to establish a proper model, where the membrane performance varies with operation conditions. To demonstrate the significant advantages of the VP membrane, a NaA zeolite membrane used in industry was characterized to establish the separation model of a VP membrane, which was later used to couple with different distillation techniques (a single column versus three columns) in process simulation to probe the cost-effectiveness for production of fuel ethanol from fermentation broth based on the gas feeding condition. The obtained energy consumptions were also used to compare with the conventional separation technique—PSA, respectively, and the results indicated that the energy efficiency of the distillation—VP coupling was consistently higher than that with the distillation—PSA coupling. On the basis of a multieffect distillation technique, the coupling of three columns with a VP membrane yielded the highest separation efficiency. The results showed that only 2.7 tons of steam per ton of fuel ethanol were consumed using a 3.0 wt % ethanol broth, which saved 0.25 tons than the results by distillation—PSA coupling. The excess of the steam in distillation—PSA coupling could be attributed to the higher ethanol concentration of the distill (92 wt %) from the HP column, and an additional recycling sweep flow, which had to be sufficiently high to fulfill the operation for the adsorption unit. The dependences of the energy consumption on the ethanol concentration of the feed were also analyzed for the distillation coupling with VP membranes and the PSA unit, respectively, which suggested that the ethanol content was a decisive factor to determine the steam consumption in the coupling techniques. To further explore the relationship between the energy consumption and operation conditions, the variation of operation pressure in the LP and HP columns versus split ratio was systematically analyzed. The results indicated that the pressure in the LP column exerted significant influence on the split ratio of FS1, so the pressure of the HP column is preferably adjusted according to practical production due to fewer fluctuations in the system. This conclusion was

further supported by the detailed mass flow rates at the top and bottoms of the columns, which were almost unchanged during the pressure adjustment in the HP column.

■ ASSOCIATED CONTENT

Supporting Information

The Supporting Information is available free of charge at <https://pubs.acs.org/doi/10.1021/acs.iecr.1c01978>.

Energy consumption analysis on the dissolved CO₂ in feed, detailed stream information, and modeling methods (PDF)

■ AUTHOR INFORMATION

Corresponding Authors

Xuechao Gao — State Key Laboratory of Materials-Oriented Chemical Engineering, College of Chemical Engineering, Nanjing Tech University, Nanjing 211816, P. R. China; orcid.org/0000-0001-5925-8127; Phone: (86)25-83172268; Email: xuechao.gao@njtech.edu.cn; Fax: (86)25-83172268

Xuehong Gu — State Key Laboratory of Materials-Oriented Chemical Engineering, College of Chemical Engineering, Nanjing Tech University, Nanjing 211816, P. R. China; orcid.org/0000-0001-9953-0076; Phone: (86)25-83172268; Email: xhgu@njtech.edu.cn; Fax: (86)25-83172268

Authors

Jiacheng Wang — State Key Laboratory of Materials-Oriented Chemical Engineering, College of Chemical Engineering, Nanjing Tech University, Nanjing 211816, P. R. China

Jiaqi Zhang — State Key Laboratory of Materials-Oriented Chemical Engineering, College of Chemical Engineering, Nanjing Tech University, Nanjing 211816, P. R. China

Zhou Hong — Nanjing Membrane Materials Industrial Technology Research Institute Co., Ltd, Nanjing 211808, P. R. China

Complete contact information is available at: <https://pubs.acs.org/doi/10.1021/acs.iecr.1c01978>

Notes

The authors declare no competing financial interest.

■ ACKNOWLEDGMENTS

This work is sponsored by the National Natural Science Foundation of China (22035002, 22178166, and 21808106), National Key Research and Development Project of China (2018YFE0118200, 2021YFC2101201), Jiangsu Provincial Policy Guidance Project (International/Hong Kong, Macau and Taiwan Cooperation of Science and Technology): One-Belt-One-Road Innovative Program (BZ2020065). The computational resources generously provided by the High-Performance Computing Center of Nanjing Tech University are greatly appreciated.

■ REFERENCES

- (1) Farrell, A. E.; Plevin, R. J.; Turner, B. T.; Jones, A. D.; O'Hare, M.; Kammen, D. M. Ethanol Can Contribute to Energy and Environmental Goals. *Science* **2006**, *311* (5760), 506.
- (2) Kerr, R. A.; Service, R. F. What can replace cheap oil - and when? *Science* **2005**, *309* (5731), 101.
- (3) Widagdo, S.; Seider, W. D. Journal review. Azeotropic distillation. *AIChE J.* **1996**, *42* (1), 96–130.

- (4) Zhang, X.; Ning, Z.; Wang, D. K.; Diniz da Costa, J. C. A novel ethanol dehydration process by forward osmosis. *Chem. Eng. J.* **2013**, *232*, 397–404.
- (5) Kaminski, W.; Marszałek, J.; Ciolkowska, A. Renewable energy source - Dehydrated ethanol. *Chem. Eng. J.* **2008**, *135* (1), 95–102.
- (6) Schubert, C. Can biofuels finally take center stage? *Nat. Biotechnol.* **2006**, *24* (7), 777–784.
- (7) Somerville, C. The Billion-Ton Biofuels Vision. *Science* **2006**, *312* (5778), 1277.
- (8) Shi, J.; Sharma-Shivappa, R. R.; Chinn, M.; Howell, N. Effect of microbial pretreatment on enzymatic hydrolysis and fermentation of cotton stalks for ethanol production. *Biomass Bioenergy* **2009**, *33* (1), 88–96.
- (9) Zhang, W.; Lin, Y.; Zhang, Q.; Wang, X.; Wu, D.; Kong, H. Optimisation of simultaneous saccharification and fermentation of wheat straw for ethanol production. *Fuel* **2013**, *112*, 331–337.
- (10) Kazi, F. K.; Fortman, J. A.; Anex, R. P.; Hsu, D. D.; Aden, A.; Dutta, A.; Kothandaraman, G. Techno-economic comparison of process technologies for biochemical ethanol production from corn stover. *Fuel* **2010**, *89*, S20–S28.
- (11) Stephanopoulos, G. Challenges in Engineering Microbes for Biofuels Production. *Science* **2007**, *315* (5813), 801.
- (12) Gomis, V.; Pedraza, R.; Saquete, M. D.; Font, A.; García-Cano, J. Ethanol dehydration via azeotropic distillation with gasoline fractions as entrainers: A pilot-scale study of the manufacture of an ethanol–hydrocarbon fuel blend. *Fuel* **2015**, *139*, 568–574.
- (13) Singh, A.; Rangaiah, G. P. Review of Technological Advances in Bioethanol Recovery and Dehydration. *Ind. Eng. Chem. Res.* **2017**, *56* (18), 5147–5163.
- (14) Feng, X.; Huang, R. Y. M. Liquid Separation by Membrane Pervaporation: A Review. *Ind. Eng. Chem. Res.* **1997**, *36* (4), 1048–1066.
- (15) Gascon, J.; Kapteijn, F.; Zornoza, B.; Sebastián, V.; Casado, C.; Coronas, J. Practical Approach to Zeolitic Membranes and Coatings: State of the Art, Opportunities, Barriers, and Future Perspectives. *Chem. Mater.* **2012**, *24* (15), 2829–2844.
- (16) Chapman, P. D.; Oliveira, T.; Livingston, A. G.; Li, K. Membranes for the dehydration of solvents by pervaporation. *J. Membr. Sci.* **2008**, *318* (1), 5–37.
- (17) Caro, J.; Noack, M.; Kölsch, P. Zeolite membranes: From the laboratory scale to technical applications. *Adsorption* **2005**, *11* (3), 215–227.
- (18) Richter, H.; Voigt, I.; Kühnert, J.-T. Dewatering of ethanol by pervaporation and vapour permeation with industrial scale NaA-membranes. *Desalination* **2006**, *199* (1), 92–93.
- (19) Pina, M. P.; Mallada, R.; Arruebo, M.; Urbiztondo, M.; Navascués, N.; de la Iglesia, O.; Santamaria, J. Zeolite films and membranes. Emerging applications. *Microporous Mesoporous Mater.* **2011**, *144* (1), 19–27.
- (20) Caro, J.; Noack, M. Zeolite membranes - Recent developments and progress. *Microporous Mesoporous Mater.* **2008**, *115* (3), 215–233.
- (21) Liu, Y.; Yang, Z.; Yu, C.; Gu, X.; Xu, N. Effect of seeding methods on growth of NaA zeolite membranes. *Microporous Mesoporous Mater.* **2011**, *143* (2), 348–356.
- (22) Yang, Z.; Liu, Y.; Yu, C.; Gu, X.; Xu, N. Ball-milled NaA zeolite seeds with submicron size for growth of NaA zeolite membranes. *J. Membr. Sci.* **2012**, *392–393*, 18–28.
- (23) Yu, C.; Liu, Y.; Chen, G.; Gu, X.; Xing, W. Pretreatment of Isopropanol Solution from Pharmaceutical Industry and Pervaporation Dehydration by NaA Zeolite Membranes. *Chin. J. Chem. Eng.* **2011**, *19* (6), 904–910.
- (24) Yu, C.; Zhong, C.; Liu, Y.; Gu, X.; Yang, G.; Xing, W.; Xu, N. Pervaporation dehydration of ethylene glycol by NaA zeolite membranes. *Chem. Eng. Res. Des.* **2012**, *90* (9), 1372–1380.
- (25) Liu, D.; Zhang, Y.; Jiang, J.; Wang, X.; Zhang, C.; Gu, X. High-performance NaA zeolite membranes supported on four-channel ceramic hollow fibers for ethanol dehydration. *RSC Adv.* **2015**, *5* (116), 95866–95871.
- (26) Ji, M.; Gao, X.; Wang, X.; Zhang, Y.; Jiang, J.; Gu, X. An ensemble synthesis strategy for fabrication of hollow fiber T-type zeolite membrane modules. *J. Membr. Sci.* **2018**, *563*, 460–469.
- (27) Wang, J.; Gao, X.; Ji, G.; Gu, X. CFD simulation of hollow fiber supported NaA zeolite membrane modules. *Sep. Purif. Technol.* **2019**, *213*, 1–10.
- (28) Wee, S. L.; Tye, C. T.; Bhatia, S. Process optimization studies for the dehydration of alcohol–water system by inorganic membrane based pervaporation separation using design of experiments (DOE). *Sep. Purif. Technol.* **2010**, *71* (2), 192–199.
- (29) Peshev, D.; Livingston, A. G. OSN Designer, a tool for predicting organic solvent nanofiltration technology performance using Aspen One, MATLAB and CAPE OPEN. *Chem. Eng. Sci.* **2013**, *104*, 975–987.
- (30) Vane, L. M.; Alvarez, F. R.; Huang, Y.; Baker, R. W. Experimental validation of hybrid distillation-vapor permeation process for energy efficient ethanol–water separation. *J. Chem. Technol. Biotechnol.* **2009**, *85* (4), 502–511.
- (31) Vane, L. M.; Alvarez, F. R.; Rosenblum, L.; Govindaswamy, S. Efficient ethanol recovery from yeast fermentation broth with integrated distillation - Membrane process. *Ind. Eng. Chem. Res.* **2013**, *52* (3), 1033–1041.
- (32) Singh, A.; Rangaiah, G. P. Development and optimization of a novel process of double-effect distillation with vapor recompression for bioethanol recovery and vapor permeation for bioethanol dehydration. *J. Chem. Technol. Biotechnol.* **2019**, *94* (4), 1041–1056.
- (33) Singh, A.; da Cunha, S.; Rangaiah, G. P. Heat-pump assisted distillation versus double-effect distillation for bioethanol recovery followed by pressure swing adsorption for bioethanol dehydration. *Sep. Purif. Technol.* **2019**, *210*, 574–586.
- (34) Singh, A.; Rangaiah, G. P. Process Development and Optimization of Bioethanol Recovery and Dehydration by Distillation and Vapor Permeation for Multiple Objectives. In *Differential Evolution in Chemical Engineering*; World Scientific: 2016; Vol. 6, pp 289–320.
- (35) Pettersen, T.; Lien, K. M. Design of hybrid distillation and vapor permeation processes. *J. Membr. Sci.* **1995**, *102*, 21–30.
- (36) Vane, L. M. Separation technologies for the recovery and dehydration of alcohols from fermentation broths. *Biofuels, Bioproducts and Biorefining* **2008**, *2* (6), 553–588.
- (37) Morigami, Y.; Kondo, M.; Abe, J.; Kita, H.; Okamoto, K. The first large-scale pervaporation plant using tubular-type module with zeolite NaA membrane. *Sep. Purif. Technol.* **2001**, *25* (1), 251–260.
- (38) Rangnekar, N.; Mittal, N.; Elyassi, B.; Caro, J.; Tsapatsis, M. Zeolite membranes – a review and comparison with MOFs. *Chem. Soc. Rev.* **2015**, *44* (20), 7128–7154.
- (39) Harvianto, G. R.; Ahmad, F.; Nhien, L. C.; Lee, M. Vapor permeation-distillation hybrid processes for cost-effective isopropanol dehydration: modeling, simulation and optimization. *J. Membr. Sci.* **2016**, *497*, 108–119.
- (40) Gao, X.; Wang, S.; Wang, J.; Xu, S.; Gu, X. The study on the coupled process of column distillation and vapor permeation by NaA zeolite membrane for ethanol dehydration. *Chem. Eng. Res. Des.* **2019**, *150*, 246–253.
- (41) Zhang, Y.; Du, P.; Shi, R.; Hong, Z.; Zhu, X.; Gao, B.; Gu, X. Blocking defects of zeolite membranes with WS2 nanosheets for vapor permeation dehydration of low water content isopropanol. *J. Membr. Sci.* **2020**, *597*, 117625.
- (42) Sato, K.; Sugimoto, K.; Nakane, T. Preparation of higher flux NaA zeolite membrane on asymmetric porous support and permeation behavior at higher temperatures up to 145°C in vapor permeation. *J. Membr. Sci.* **2008**, *307* (2), 181–195.
- (43) Li, H.; Guo, C.; Guo, H.; Yu, C.; Li, X.; Gao, X. Methodology for design of vapor permeation membrane-assisted distillation processes for aqueous azeotrope dehydration. *J. Membr. Sci.* **2019**, *579*, 318–328.
- (44) Koch, K.; Górak, A. Pervaporation of binary and ternary mixtures of acetone, isopropyl alcohol and water using polymeric

membranes: Experimental characterisation and modelling. *Chem. Eng. Sci.* **2014**, *115*, 95–114.

(45) Koch, K.; Sudhoff, D.; Kreiß, S.; Górak, A.; Kreis, P. Optimisation-based design method for membrane-assisted separation processes. *Chem. Eng. Process.* **2013**, *67*, 2–15.

(46) Caballero, J. A.; Grossmann, I. E.; Keyvani, M.; Lenz, E. S. Design of Hybrid Distillation–Vapor Membrane Separation Systems. *Ind. Eng. Chem. Res.* **2009**, *48* (20), 9151–9162.

(47) Luyben, W. L. Control of a Column/Pervaporation Process for Separating the Ethanol/Water Azeotrope. *Ind. Eng. Chem. Res.* **2009**, *48* (7), 3484–3495.

(48) Servel, C.; Roizard, D.; Favre, E.; Horbez, D. Improved Energy Efficiency of a Hybrid Pervaporation/Distillation Process for Acetic Acid Production: Identification of Target Membrane Performances by Simulation. *Ind. Eng. Chem. Res.* **2014**, *53* (18), 7768–7779.

(49) Verhoef, A.; Degève, J.; Huybrechs, B.; van Veen, H.; Pex, P.; Van der Bruggen, B. Simulation of a hybrid pervaporation–distillation process. *Comput. Chem. Eng.* **2008**, *32* (6), 1135–1146.

(50) de Medeiros, E. M.; Noorman, H.; Maciel Filho, R.; Posada, J. A. Production of ethanol fuel via syngas fermentation: Optimization of economic performance and energy efficiency. *Chem. Eng. Sci.* **2020**, *5*, 100056.

(51) Almeida Benalcázar, E.; Noorman, H.; Maciel Filho, R.; Posada, J. A. Modeling ethanol production through gas fermentation: a biothermodynamics and mass transfer-based hybrid model for microbial growth in a large-scale bubble column bioreactor. *Biotechnol. Biofuels* **2020**, *13* (1), 59.

(52) Wang, X.; Liao, B.; Li, Z.; Liu, G.; Diao, L.; Qian, F.; Yang, J.; Jiang, Y.; Zhao, S.; Li, Y.; Yang, S. Reducing glucoamylase usage for commercial-scale ethanol production from starch using glucoamylase expressing *Saccharomyces cerevisiae*. *Bioresour. Bioprocess.* **2021**, *8* (1), No. 20 DOI: 10.1186/s40643-021-00375-5.

(53) Bai, F. W.; Anderson, W. A.; Moo-Young, M. Ethanol fermentation technologies from sugar and starch feedstocks. *Biotechnol. Adv.* **2008**, *26* (1), 89–105.

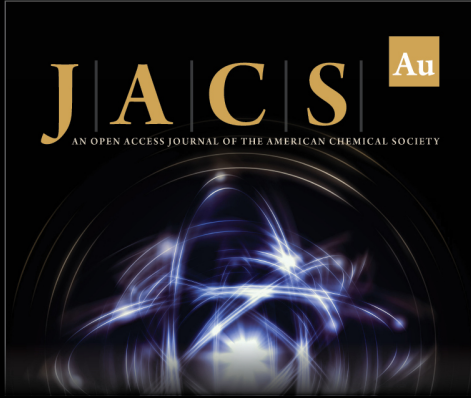
(54) Matsukata, M.; Sawamura, K.-i.; Sekine, Y.; Kikuchi, E. Review on Prospects for Energy Saving in Distillation Process with Microporous Membranes. In *Membrane Science and Technology*; Oyama, S. T., Stagg-Williams, S. M., Eds.; Elsevier: 2011; Vol. 14, Chapter 8, pp 175–193.

(55) Palacios-Bereche, R.; Ensinas, A. V.; Modesto, M.; Nebra, S. A. Double-effect distillation and thermal integration applied to the ethanol production process. *Energy* **2015**, *82*, 512–523.

(56) Carmo, M. J.; Gubulin, J. C. Ethanol-Water Separation in the PSA Process. *Adsorption* **2002**, *8* (3), 235–248.


(57) Zhu, W.; Gora, L.; van den Berg, A. W. C.; Kapteijn, F.; Jansen, J. C.; Moulijn, J. A. Water vapour separation from permanent gases by a zeolite-4A membrane. *J. Membr. Sci.* **2005**, *253* (1), 57–66.


(58) Errico, M.; Rong, B.-G.; Tola, G.; Spano, M. Optimal Synthesis of Distillation Systems for Bioethanol Separation. Part 2. Extractive Distillation with Complex Columns. *Ind. Eng. Chem. Res.* **2013**, *52* (4), 1620–1626.



JACS Au
AN OPEN ACCESS JOURNAL OF THE AMERICAN CHEMICAL SOCIETY

Editor-in-Chief
Prof. Christopher W. Jones
Georgia Institute of Technology, USA

Open for Submissions 

pubs.acs.org/jacsau  ACS Publications
Most Trusted. Most Cited. Most Read.